Molecular dynamics simulations reveal the conformational flexibility of Lipid II and its loose association with the defensin plectasin in the *Staphylococcus aureus* membrane.

Sarah Witzke[1,2] *, Michael Petersen*[1]*, Timothy S. Carpenter*[3*] *and Syma Khalid*[2*]

[1] Department of Physics, Chemistry and Pharmacy
University of Southern Denmark
Denmark

[2] School of Chemistry,
University of Southampton,
Highfield,
Southampton,
SO17 1BJ,
UK.

[3] Biosciences and Biotechnology Division,
Lawrence Livermore National Laboratory,
7000 East Avenue,
Livermore,
CA,
USA.

[*]To whom correspondence should be addressed: S.Khalid@soton.ac.uk or carpenter36@llnl.gov

Abbreviations and Textual Footnotes

ADPG	Tetra-anteiso-myristoyl Cardiolipin
Ala	Alanine
ALPG	Lysyl-AMPG
AMPG	1,2-di-anteiso-myristoyl-*sn*-glycero-3-phosphoglycerol
Cys	Cysteine
DMPG	1,2-dimyristoyl-*sn*-glycero-3-phosphoglycerol
DPC	Dodecylphosphocholine
Glc	*N*-acetylglucosamine
Gly	Glycine
His	Histidine
LII	Lipid II
Lys	Lysine
MD	Molecular Dynamics
Mur	*N*-acetylmuramic acid
PG	Phosphatidylglycerol
Phe	Phenylalanine
RDF	Radial Distribution Function
S. aureus	*Staphylococcus aureus*
SI	Supporting Information

Abstract

Lipid II is a precursor for peptidoglycan, which is the main component of the bacterial cell wall. Lipid II is a relatively conserved and important part of the cell wall biosynthesis pathway and is targeted by antibiotics such as the lantibiotics, which achieve their function by disrupting the biosynthesis of the cell wall. Given the urgent need for development of novel antibiotics to counter the growing threat of bacterial infection, it is imperative that a thorough molecular-level characterisation of the molecules targeted by antibiotics is achieved. To this end, we present a molecular dynamics simulation study of the conformational dynamics of Lipid II within a detailed model of the *Staphylococcus aureus* cell membrane. We show that Lipid II is able to adopt a range of conformations, even within the packed lipidic environment of the membrane. Our simulations also reveal dimerization of Lipid II mediated by cations. In the presence of the defensin peptide plectasin, the conformational lability of Lipid II enables it to form loose complexes with the protein, *via* a number of different binding modes.

Introduction

Lipid II is a key component in the synthesis of the peptidoglycan layer outside the plasma membrane of all bacteria, where Lipid II molecules carry the peptidoglycan building blocks from the inside of the cell to the outside. When the building block has been incorporated into the growing peptidoglycan, Lipid II is released and recycled in another round of transportation. Lipid II thus represents a bottleneck in peptidoglycan biogenesis. The importance of Lipid II as a target for antimicrobial peptides is seen with the glycopeptide vancomycin, that since its discovery has been reserved as a last resort drug against resistant strains.[1] Vancomycin binds the D-Ala–D-Ala moiety (see Figure 1) of Lipid II and thereby 'trapping' Lipid II and rendering it unable to partake in further synthesis of peptidoglycan. Unfortunately bacterial resistance towards vancomycin is increasing. Vancomycin cannot form a stable complex with Lipid II when the D-Ala–D-Ala moiety of the latter has been mutated into D-Ala-D-Lactate.[2] Another antimicrobial peptide that targets Lipid II is the lantibiotic nisin. Nisin binds to the pyrophosphate group (see Figure 1) of Lipid II, and it is therefore hoped that bacterial resistance to nisin is less likely to arise due to the pivotal role of the pyrophosphate moiety which cannot easily be mutated into another form while still maintaining the function of Lipid II.[3] Another recently identified promising antibiotic, Teixobactin, also targets the pyrophosphate group of Lipid II.[4]

A promising new candidate for a Lipid II targeting antimicrobial peptide is the defensin plectasin. Defensins are short, cysteine-rich, cationic peptides that form part of the innate immune response system in vertebrates and invertebrates and have also been found in plants. They function as host defence peptides against bacteria, fungi, and many types of viruses. Plectasin is a 40–amino acid fungal defensin produced by the saprophytic ascomycete *Pseudoplectania nigrella*.[5] It has been shown to be potent against several Gram-positive bacteria, for instance *Streptococcus pneumonia* and *Staphylococcus aureus* (*S. aureus*).[5,6] Plectasin is composed of one α-helix and two β-strands stabilised by three disulfide bonds, this architecture closely resembles that of many other defensins from spiders, scorpions, and mussels.[5] The mechanism of action of defensins was initially proposed to arise from the amphipathic nature of the peptides enabling them to bind to

and disrupt the membranes of the host cells. However in contrast to this general mechanism, a recent combined experimental and computational study has suggested that plectasin binds directly to Lipid II[7] and therefore, despite its amphipathic nature, it does not compromise membrane integrity. Schneider *et al.*[7] used NMR titrations to probe the interactions between Lipid II and plectasin, and based on these results they proposed a binding mechanism through the pyrophosphate group of Lipid II. The binding to a specific target instead of a general interaction with the membrane is corroborated by a study finding that only the L-enantiomer and not the D-enantiomer of plectasin is active against Gram-positive bacteria.[8] The binding of plectasin to Lipid II instead of indiscriminate disruption of the cell membrane has two significant advantages, firstly the risk of non-specific toxicity is reduced and secondly if the recognition motif is indeed the pyrophosphate group it will decrease the potential of developing resistance.

The spread of infectious diseases and the increase in antibiotic resistance represents a life-threatening global development that calls for new approaches to control microorganisms. A better understanding of the mechanisms of antimicrobial action and how resistance towards antimicrobial agents arises is therefore needed. Computer simulations offer insight into a molecular level not easily obtained through experiments and are thus an obvious method to aid the understanding of antimicrobial actions.

Here we report an atomistic molecular dynamics study (I have deleted ‘of’) to investigate the behaviour of Lipid II in two different environments; (1) (I have deleted ‘in’) a model *S. aureus* membrane, and (2) the same membrane model interacting with the defensin peptide, plectasin. We show that Lipid II can adopt a range of conformations in a model of the *S. aureus* cell membrane, causes local rearrangement of specific lipid types, and can form cation-bridged dimers. Our results suggest loose association with plectasin with multiple binding modes available for the peptide-lipid interaction.

Methods

Atomistic molecular dynamics simulations were performed to study the dynamics of Lipid II in a model *S. aureus* membrane and also its interactions with the peptide, plectasin.

Simulation Systems

The simulations described in this paper are summarized in Table 1 - Table 2. All systems were neutralised with either Na^+ or Cl^- ions according to the total charge of the system. The systems were solvated with at least 60 water molecules per lipid. The water model used was TIP3P.[9]

S. aureus membrane

A symmetric lipid bilayer, containing 100 1,2-dimyristoyl-*sn*-glycero-3-phosphoglycerol (DMPG) lipid molecules in each leaflet, was built with the CHARMM-GUI Membrane Builder.[10] An in-house script was used to replace the DMPG lipids with specific lipids from the *S. aureus* cell membrane, using the same composition as previously reported[11] and corresponding to experimental studies:[12-14] 54% phosphatidylglycerol (PG), 36% lysyl-phosphatidylglycerol (lysyl-PG) and 10% diphosphatidylglycerol (also known as cardiolipin). All lipids are modelled with anteiso-myristoyl chains, i.e. a myristoyl (14:0) chain with a methyl branch on the second last methylene carbon. The PG lipids are henceforth named 'AMPG', while the lysyl-PG lipids are named 'ALPG' and the cardiolipins are named ADPG. The chemical structures of the lipids are shown in Figure 1 a). The CHARMM36 force field[15-24] was used, full details of the lipid models are provided in the SI.

Lipid II

Lipid II consists of a polar headgroup and a lipophilic anchor, see Figure 1. The anchor is a bactoprenol consisting of 11 isoprene units where the first seven units are in the (*Z*)-configuration and the following three are in the (*E*)-configuration.[1,25-28] The bactoprenol is longer than the hydrophobic thickness of the membrane and it has been hypothesized that this together with the inherent elasticity offered by the isoprene units allow the Lipid II molecule to change its vertical position in the membrane during the different steps of the cell wall synthesis.[28] A pyrophosphate group links the bactoprenol tail to a *N*-acetylglucosamine (GlcNAc) sugar, which itself is linked to a *N*-acetylmuramic acid (MurNac) sugar. The sugar moieties are henceforth referred to as Glc and Mur, respectively. A peptide sidechain is linked to Glc, the nature of which is bacterial species

dependent. In this study we use a penta-peptide of the amino acids L-Ala–γ-D-Glu–L-Lys–D-Ala–D-Ala that has been used in several other studies.[5,7,29-32] The peptidoglycan of *S. aureus* also contain a pentaglycin interpeptide bridge[33] attached to the Lys residue, but this was omitted both for simplicity and to be consistent with other studies.[5,7,30-32] Full details of the model are provided in the SI.

The VMD graphics package[34] was used to position the Lipid II molecule(s) in a transmembrane orientation within the *S. aureus* membrane. For the simulations of two Lipid II molecules in the same membrane, the Lipid II molecules were originally positioned approximately parallel to each other in the membrane with 10 Å between the tails, 20 Å between the two pyrophosphate groups, and 11.7 Å as the shortest distance between the two head groups.

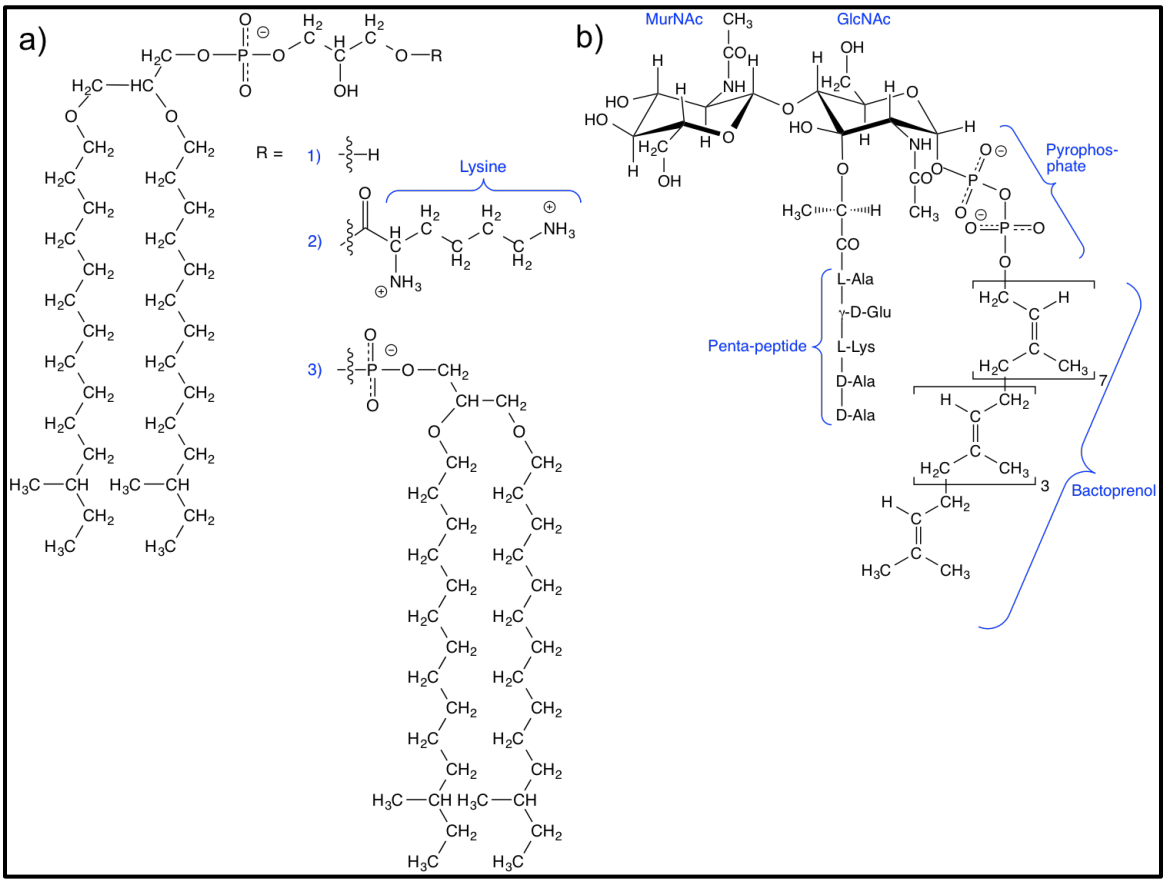

Figure 1 Chemical structure of a) The three lipid types used in the *S. aureus* model membrane: 1) AMPG, 2) ALPG and 3) ADPG, and b) Lipid II. MurNAc: *N*-acetylmuramic acid, GlcNAc: *N*-acetylglucosamine.

Plectasin

The coordinates of the complex of plectasin and the Lipid II headgroup produced by docking calculations[35] were obtained from Alexandre Bonvin. The Lipid II in this complex only had a short tail of three isoprene units, therefore we modelled in the longer tail from the full Lipid II molecule to give a total of 11 isoprene units and an approximate length of 45 Å in the stretched conformation. Given the NMR experiments upon which the docking complex was based were performed at pH 6.1, the two histidine residues in plectasin were protonated on the imidazole ring.[35] We used the PROPKA 3.1 server[36,37] to determine the pK_a of the two histidine residues, and they were 6.19 (His16) and 5.37 (His18), respectively. Based on these pK_a values we initially represented both histidine residues in their neutral state. Visual inspection did not reveal a likely propensity for the nitrogen proton to be placed either on the δ-nitrogen or the ε-nitrogen, hence different systems were set up where both histidine residues were either protonated on the δ-nitrogen or the ε-nitrogen. We also simulated a system where His18 was doubly protonated (i.e. positively charged). Henceforth we will use the notation 'δ,δ' to denote that both His16 and His18 are protonated on the δ-nitrogen, 'ε,ε' to denote that both His16 and His18 are protonated on the ε-nitrogen and 'δ,P' to denote that His16 is protonated on the δ-nitrogen while His18 is doubly protonated (and hence positively charged). The plectasin-Lipid II complex was inserted into the *S. aureus* membrane using the same protocol as insertion of the uncomplexed Lipid II molecules.

Overview of Simulations

A summary of the simulations discussed in the present work is provided in Table 1 and Table 2

Table 1 Simulations of Lipid II in a *S. aureus* model membrane. a: Simulation run with Amber. b: Simulation run with NAMD.

#Lipid II molecules	0		1				2			
Temperature [K]	313	313	313	313	320	320	325	325	325	325
Sim. time [ns]	245[a]	342[a]	300[a]	300[a]	200[b]	200[b]	200[b]	200[b]	300[b]	300[b]

Table 2 Simulations of Lipid II and plectasin in a *S. aureus* model membrane. δ: Neutral histidine with proton in δ-position. ε: Neutral histidine with proton in ε-position. P: Positively charged histidine, protons in both δ- and ε-positions. a: Positional restraints on the plectasin-Lipid II complex. b: Distance restraints between plectasin and Lipid II. c: These three simulations were started from the same restrained structure. d: Simulation run with Amber. e: Simulation run with NAMD.

Protonation of His 16,18	δ,δ		ε,ε							δ,P
Temperature [K]	313	313	313	313	313	313	313	313	313	313
Sim. w. restraints [ns]	0	0	21[a]	17[b]	20[b]	1[b,c]	1[b,c]	1[b,c]	10[a]	0
Sim. w/o. restraints [ns]	200[e]	200[e]	96[d]	0[d]	12[d]	18[d]	30[d]	21[d]	132[e]	200[d]

Simulation Parameters and Protocol

The MD simulations were performed with either the MD packages Amber 12,[38] Amber 14,[39] or NAMD[40] version 2.8 and 2.10. For the systems run in Amber we used CHAMBER[41] from the AmberTools12 or ParmEd from AmberTools15 to convert the coordinates and topology files from VMD/NAMD format into the format used in the Amber Suite of programs.

Simulations performed with Amber 12 or Amber14

The initial structures were first minimized with the steepest descent method and then the conjugate gradients method until either a total of ten thousand steps were reached or the gradient of the coordinates were less than 1.0^{-4} kcal mol^{-1} Å^{-1}. The systems were then heated gradually from 0 K to 100 K over 5 ps in the NVT ensemble. A second step of heating over 100 ps raised the temperature from 100 K to the temperature indicated in Table 1 - Table 2 as well as changing from the NVT ensemble to NPT (1.0 bar) with the Berendsen barostat[42] with anisotropic scaling and a relaxation time of 2.0 ps. During the heating, all atoms in the lipids were subjected to weak, harmonic positional restraints (force constant of 10 kcal mol^{-1} Å^{-2}). For the production run, the systems were simulated with a time step of 2 fs, constant temperature and constant anisotropic pressure at 1.0 bar

(relaxation time of 1.0 ps). For all simulations the temperature was controlled with the Langevin thermostat[43] (collision frequency of 1.0 ps^{-1}, except for the system of Lipid II with plectasin-(δ,P) where the collision frequency was 2.0 ps^{-1}). Bonds to hydrogens were constrained with SHAKE.[44] A non-bonded cut-off of 10 Å was employed and the non-bonded interactions were treated with the Particle Mesh Ewald (PME) method.[45] In the simulations in which positional restraints were applied to keep the plectasin-Lipid II complex intact, the equilibration procedure included a 10 ns simulation with a harmonic restraint applied to all atoms in plectasin and Lipid II with a force constant of 10 kcal mol^{-1} $Å^{-2}$, after which the force constant was gradually decreased over 11 ns to first 5 kcal mol^{-1} $Å^{-2}$ and then 1 kcal mol^{-1} $Å^{-2}$ before completely removing the restraints. Simulations in which distance restraints were applied to the plectasin-Lipid II complex, five hydrogen bond distances between the plectasin backbone amide protons of the residues Phe2, Gly3, Cys4 and Cys37 to the oxygens in the pyrophosphate group of Lipid II were restrained with a square-bottom well potential where the sides of the well had a force constant of 25 kcal mol^{-1} $Å^{-2}$. These hydrogen bonds are highlighted as important for the complexation of Lipid II and plectasin by Schneider *et al.* [7]

Simulations performed with NAMD 2.8 and 2.10

The initial structures were minimized for 5000 steps with conjugate gradient method, after which the systems were heated to the indicated temperature in Table 1 - Table 2 during a short NVT equilibration of 500 ps with a time step of 1 fs. Afterwards the time step was lowered to 0.5 fs and a further 500 ps equilibration was run to with the Nosé-Hoover Langevin Piston[46,47] to obtain a constant pressure of 1 atm. The pressure coupling was anisotropic but with a constant x/y ratio. The time step was then increased to 1 fs and another 500 ps of equilibration was performed, after which the time step was further increased to 2 fs for the production run. The temperature and pressure were controlled with Langevin dynamics[43] with a damping coefficient of 5 ps^{-1}, while the decay time for the Nosé-Hoover Langevin piston was 50 fs and the oscillation period was 100 fs. The cut-off for non-bonded interactions was 12 Å with a switching function applied between 10 and 12 Å. The PME[45] method was used for electrostatics, with a maximum spacing of 1 Å between grid points. All bonds to hydrogen atoms were constrained using the

SHAKE algorithm.[44] For the simulation with positional restraints applied to the plectasin-Lipid II complex, a harmonic restraint was applied to all atoms in plectasin and Lipid II with a force constant of 5 kcal mol^{-1} $Å^{-2}$.

Analysis

The analyses are performed with CPPTRAJ[48] from the AmberTools package version 12-15, VMD 1.9.2[34] and in-house scripts.

Results

Lipid II in the protein-free *S. aureus* membrane

Location and conformation of Lipid II in the *S. aureus* cell membrane

Molecular dynamics simulations provide an ideal route to investigation of the conformational dynamics of specific lipid types within complex membranes.[11] Given the paucity of experimental data of the molecular-level behavior of Lipid II within a *S. aureus* membrane, we have characterised this from our MD trajectories. Density plots reveal that the pyrophosphate group of Lipid II is on average located at the same height with respect to the membrane normal as the phosphate groups of the other membrane lipids: the maximum density is 20.3 Å above the membrane centre (defined as the midpoint between the peak in the phosphate density in either leaflet), while the maximum density of the phosphate groups of the other lipids is found ~18 Å from the membrane centre, see Figure 2.

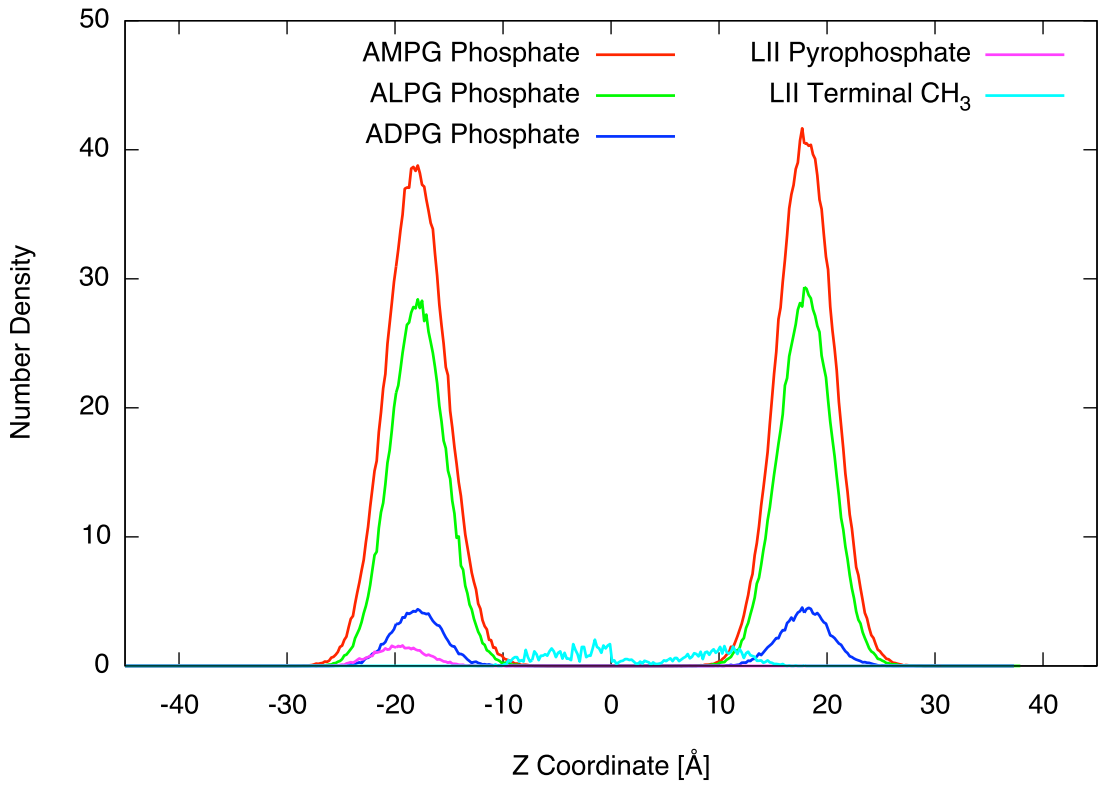

Figure 2 Number densities of the phosphate groups of the membrane lipids together with the number density of the pyrophosphate of Lipid II (LII) for one of the simulations with a single Lipid II molecule embedded in the model *S. aureus* membrane at 313 K. The other simulations of either one or two Lipid II molecules in the model *S. aureus* membrane (without plectasin) show similar number densities. The number density of the terminal CH_3 group of Lipid II has been multiplied by a factor of five to make it more visible. LII: Lipid II.

Our results reveal that the Lipid II tail samples a large conformational space and can adopt a broad range of conformations without a clear preference. This is indicated by the broad range of angles between the upper and lower part of the tail (Figure 3). Further evidence comes from the observation that the density of the terminal methyl group of the Lipid II tail in all simulations is found spread over whole range of the hydrophobic thickness of the membrane (cyan line, Figure 2). In Figure S6 in the SI is shown the Z-coordinate of the center of mass of the terminal methyl-carbons as a function of time, showing no clear preferred location of the terminal methyl groups over the time scales simulated.

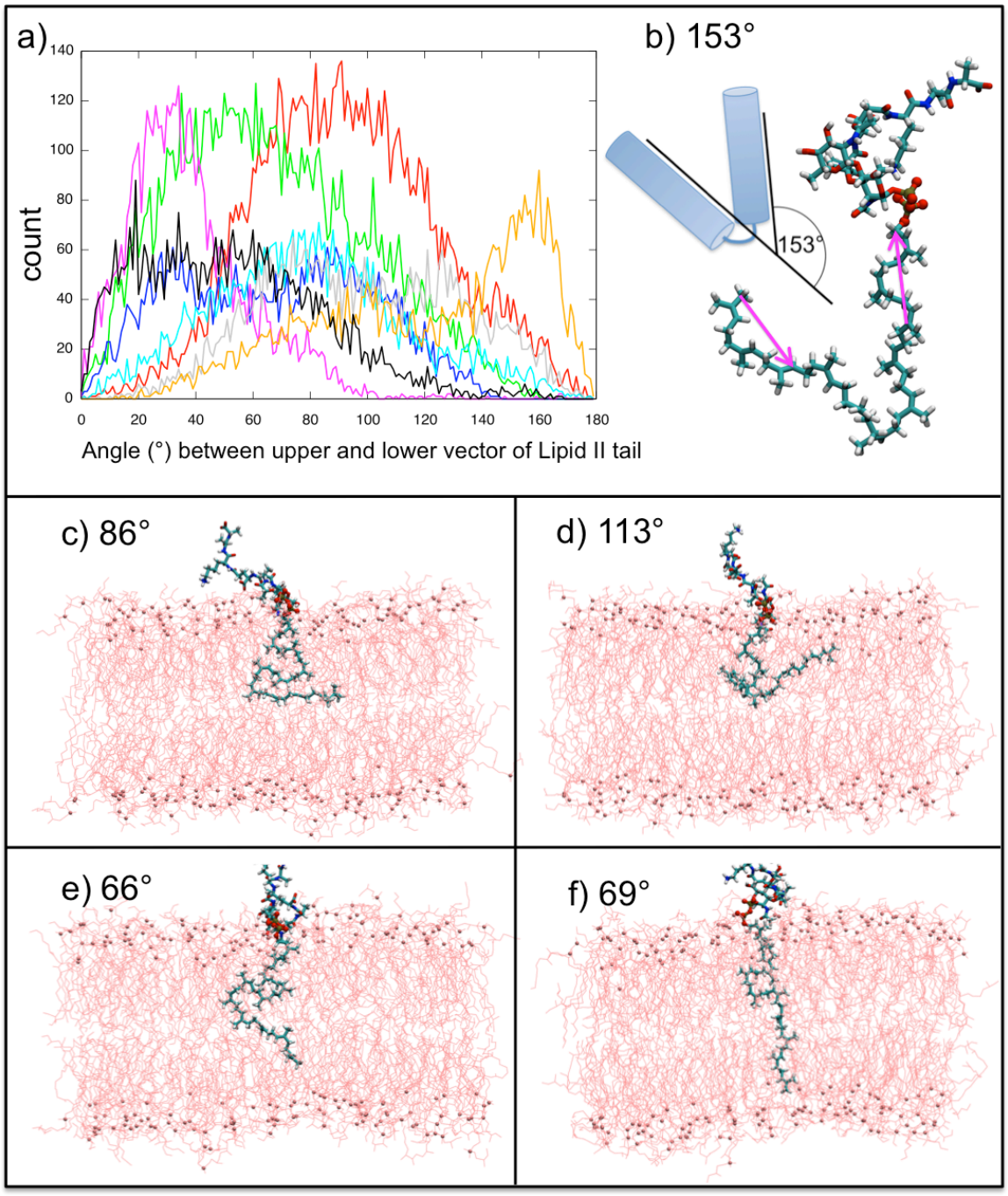

Figure 3 Conformations of the tail of Lipid II: a) Plot of the angle between the upper and the lower part of the Lipid II tail from a set of simulations performed; b) Snapshot of Lipid II with the two vectors (magenta) between which the angle in a) is calculated, this is also shown schematically with the blue cylinders; c)-f) Snapshots of different conformations of Lipid II in the *S. aureus* membrane (pink, hydrogens omitted for clarity, phosphorous atoms in the headgroups are shown as spheres). The angles between the upper and lower part of the Lipid II tail as defined by the vectors in b) are given in each figure. Lipid II: Cyan: carbon, white: hydrogen, red: oxygen, tan: phosphorous, blue: nitrogen.

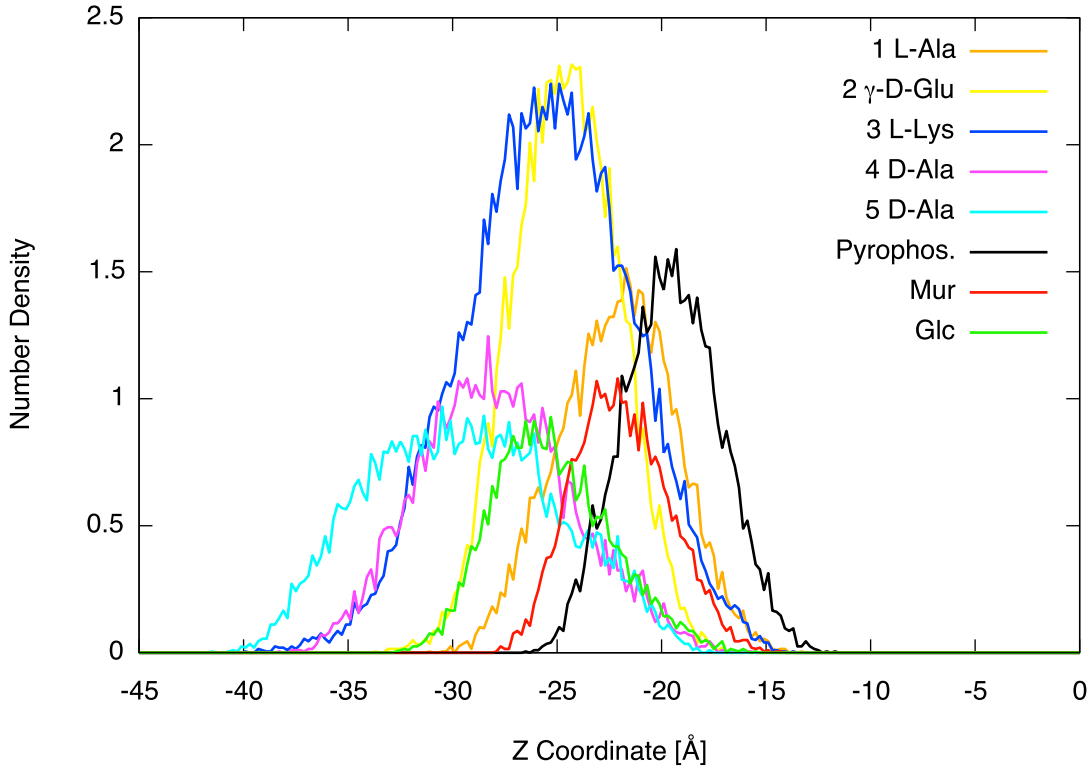

Figure 4 Representative number densities of the different parts of the Lipid II headgroup where the membrane center is at 0 Å.

Analysis of Lipid II's head group shows that it, as the tail, displays a high degree of conformational heterogeneity (Figure 4). The two sugar rings (Mur and Glc) and the first amino acid on the pentapeptide chain (1-L-Ala) are buried deep in the bilayer interface while the remaining residues on the pentapeptide chain are progressively more and more exposed to the solvent with the two distal Ala residues being fully exposed.

Interactions of Lipid II with the *S. aureus* membrane

It is instructive to characterise whether the presence of Lipid II modulates the distribution of the other lipids of the *S. aureus* membrane. We calculated the level of interaction of Lipid II with each of the lipid types comprising the membrane, in turn. Our results reveal that Lipid II has a marked preference for ALPG lipids. The positively charged lysine sidechains of the ALPG lipids interact with the pyrophosphate groups and the carboxylate group of the γ-Glu in the peptide sidechain of Lipid II, but also to a lesser extent with several of the hydroxyl oxygen atoms of the sugar moieties.

Radial distribution function (RDF) calculations were performed for each of the three lipid types around the pyrophosphate group of Lipid II, see Figure 5. The distinctive pattern of the RDF curve for ALPG around the pyrophosphate group indicates that there are hydrogen bond interactions between the ALPG lysine chain and Lipid II's headgroup. The ALPG followed by the ADPG lipids make concentric circles around Lipid II, while the AMPG lipids are almost evenly distributed. Four simulations of one Lipid II molecule in a *S. aureus* membrane were conducted (Table 1). The two simulations at 313 K started with a random distribution of the membrane lipids, while the two at 320 K were continuations of the two at 313 K. The time evolution of the number of AMPG and ALPG molecules within 5 Å of Lipid II for the two systems at 313 K indicates that the number of AMPG molecules close to Lipid II decreases, while the number of ALPG molecules increases (Figure 6). For the two systems at 320 K no change in the number of a given lipid type close to Lipid II is seen (data not shown), hence the sorting of the membrane lipids are achieved within the first 200 ns.

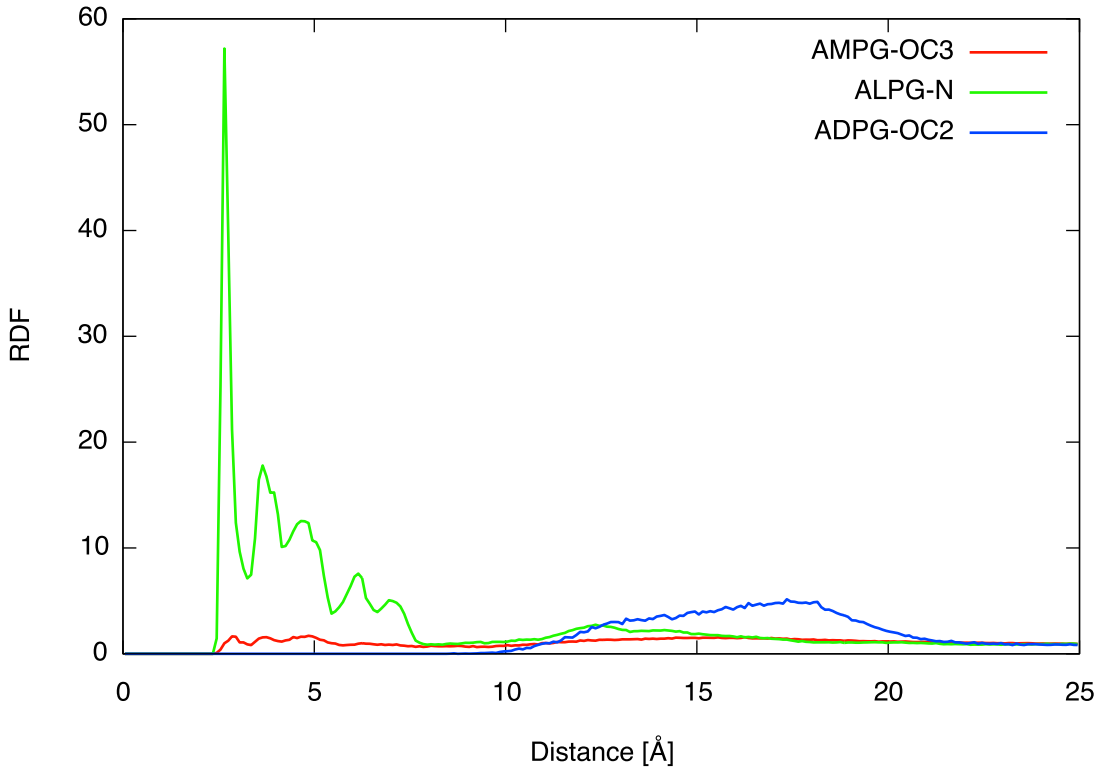

Figure 5 Representative RDF plot of each lipid type (AMPG, ALPG and ADPG) around the pyrophosphate group of Lipid II. For AMPG is used the outermost oxygen in the glycerol headgroup (OC3), for ALPG is used the nitrogen on the Cα i.e. the innermost nitrogen (N), while for ADPG is used the oxygen on the

middle carbon in the linking glycerol headgroup (OC2). The radial distribution function (RDF, or the pair correlation function) was found with a bin width of 0.1 Å and until a maximum distance of 10 Å with CPPTRAJ. The RDFs were normalized to a value of 1 when no specific ordering is taking place (i.e. in 'bulk').

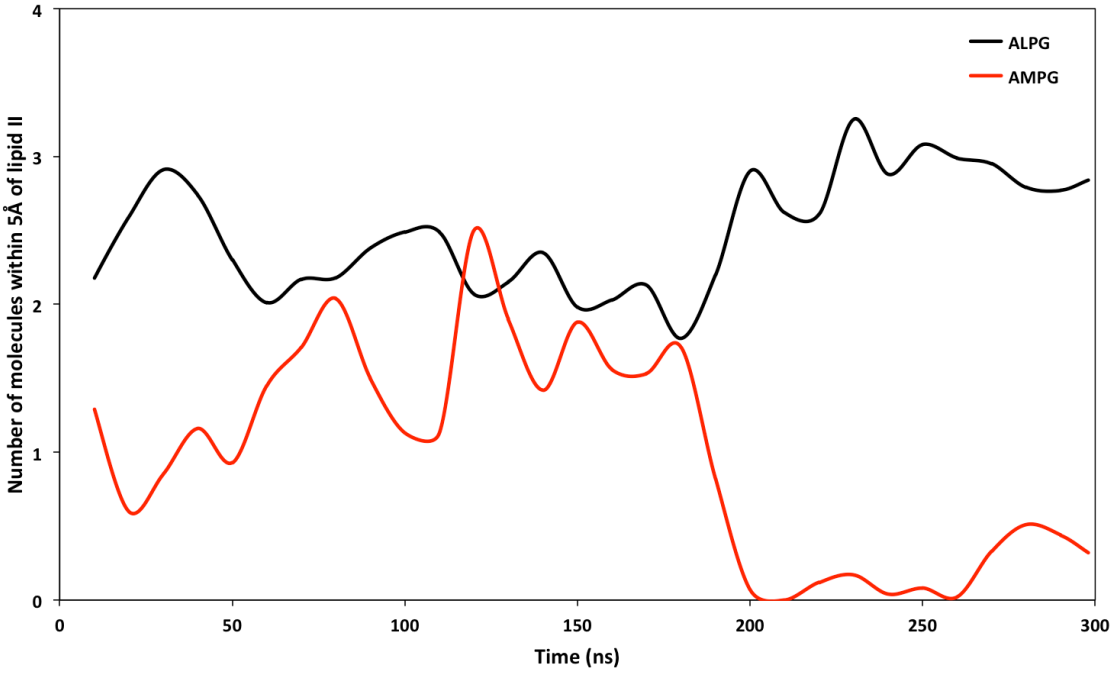

Figure 6 The number of ALPG (black line) and AMPG (red line) molecules within 5 Å of Lipid II are shown as a function of time. The values are the running averages over the two 300 ns repeat simulations starting with random distributions of membrane lipids. As the simulations progress, the lipids re-organize so that the number of ALPG molecules close to Lipid II increases, while the number of AMPG molecules close to Lipid II decreases.

Inter-Lipid II interactions

The two Lipid II molecules in the *S. aureus* membrane are initially separated such that there is 10 Å between the two approximately parallel tails, 20 Å between the two pyrophosphate groups and the shortest distance between the two head groups is 11.7 Å. We observe dimerization of the Lipid II molecules in one of the four simulations. This dimerization occurs within the first nanosecond of the simulation. The dimer is stabilised through interactions of the headgroup regions; specifically there is a hydrogen bond between one of the oxygen atoms of the pyrophosphate group in one molecule and the C6-hydroxyl group of the Mur sugar on the other Lipid II molecule. This interaction is present during the last 100 ns of the simulation. Furthermore, the free amino group on the Lys residue in the first Lipid II molecule makes several hydrogen bonds to different

hydroxyl groups (acting both as acceptor and donor) and to other oxygens in the sugars and pyrophosphate groups that can only interact as acceptors. These interactions were observed throughout the simulation and had an average lifetime (based on a cut-off distance of 3.5 Å) of less than 1 ns. A longer-lived interaction is observed between a Na^+ ion and both phosphate groups of both Lipid II molecules. Collectively, the four phosphate groups form a coordination shell around the Na^+ ion. This position is occupied by the same Na^+ ion throughout the 200 ns simulation (Figure 6). Additional Na^+ ions were also observed to form interactions with the pyrophosphate groups, but these were shorter-lived, typically up to 20 ns long at a time and did not form with all four phosphate groups simultaneously. In contrast to the headgroups, there is little interaction between the tails of the two Lipid II molecules.

In one of the other three independent simulations of the same system, the Lipid II molecules diffuse away from each other at the start of the simulation and do not interact again. In the two other simulations the two Lipid II molecules remain in the vicinity of each other: in one of the systems the two Lipid II tails remain with a minimum distance around 2-3 Å of each other for the first 240 ns, while for the remaining 60 ns there is a fluctuation back and forth in the minimum distance between 2 and 7 Å. For the other systems, the Lipid II molecules first drift apart with a minimum distance of 14 Å between them, then for around 40 ns the two tails get into contact with each other with a minimum distance of 2-6 Å. This is followed by a period of 40 ns where the two Lipid II molecules are no closer than 10 Å, after which the two peptide sidechains starts getting closer and by the end of the simulation the minimum distance of the Lipid II molecules is again 2 Å but this time it is the peptide sidechains and not the tails that interact with each other.

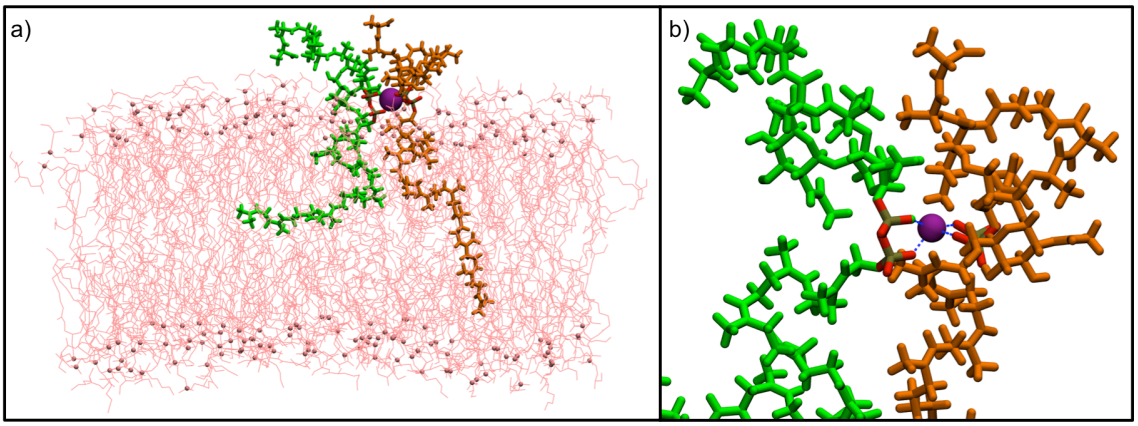

Figure 7 a) Snapshot from the simulation of two Lipid II molecules forming a 'pyrophosphate cage' around the same sodium for the entire simulation; b) Zoom of the pyrophosphate cage (size of sodium ion decreased for clarity). The two Lipid II molecules are shown in orange and green, respectively, while the oxygens and phosphorus atoms in their pyrophosphate groups are coloured red and tan, respectively. The sodium ion is shown in purple and the membrane lipdis (i.e. AMPG, ALPG and ADPG) are coloured in pink (hydrogens omitted for clarity) with their phosphorus atoms shown as spheres.

Physical properties of the membrane

The structural properties of the model *S. aureus* membrane (such as area per lipid, membrane thickness and deuterium order parameters) were largely independent of both temperature (within the range 313-325 K) and the presence of Lipid II. The data provided in Table 3 show that the area per lipid increased only slightly from an average of 62.4 $Å^2$ to an average of 63.9 $Å^2$ as the temperature was raised from 313 K to 325 K. This increase is particularly small considering that there is incorporation of first one and then two Lipid II molecules in the S. *aureus* membrane, and that this insertion alone would be expected to increase the area per lipid. The increase in temperature also results in a slight overall decrease in the deuterium order parameter of the lipid tails, see Figure 8, but given the added molecule(s) and the temperature increase, the effect is surprisingly small. Similarly, the membrane thickness is virtually unaltered in all the systems, the range being 35.9 Å to 36.2 Å.

Table 3 Time averaged area per lipid [Å^2] (each ADPG is counted as two molecules in this regard) and membrane thickness [Å] for the *S. aureus* model membrane. Standard deviations are given for both the area per lipid and membrane thickness.

#Lipid II	Temp. [K]	Area [Å^2]	Thickness [Å]
0	313	62.1 ± 0.9	36.2 ± 0.4
0	313	62.6 ± 0.8	35.9 ± 0.4
1	313	63.1 ± 0.8	36.0 ± 0.4
1	313	62.8 ± 1.0	36.0 ± 0.5
1	320	62.7 ± 0.9	36.3 ± 0.4
1	320	62.5 ± 1.0	36.3 ± 0.4
2	325	64.0 ± 0.8	36.0 ± 0.4
2	325	64.0 ± 0.9	36.0 ± 0.5
2	325	63.8 ± 0.8	36.1 ± 0.4
2	325	63.7 ± 0.9	36.1 ± 0.4

(The number of significant digits have been reduced)

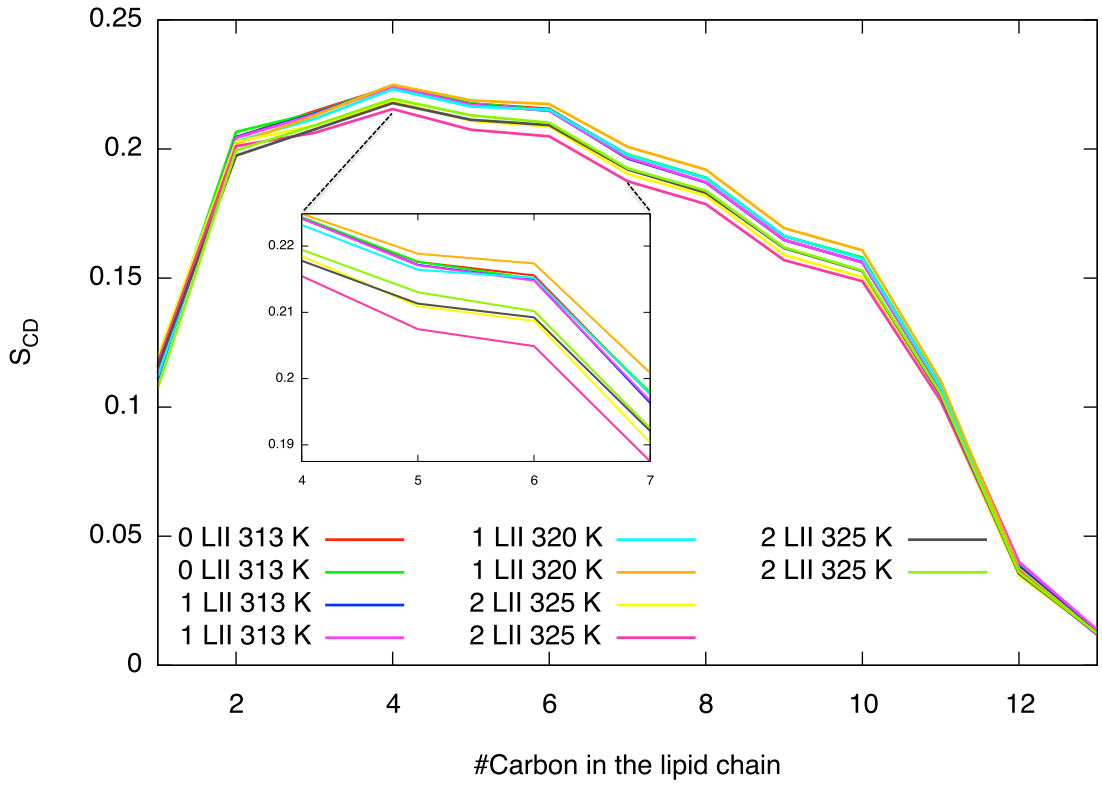

Figure 8 Deuterium order parameters for the carbon atoms of the *sn*-1 tail of the AMPG lipids in the *S. aureus* membrane simulations. Insert: Zoom of the curves from carbon number 4 to number 7. LII: Lipid II.

The average deuterium order parameter (S_{CD}) for each lipid type was calculated to investigate whether these had any dependence on the distance from the Lipid II molecule(s). The AMPG lipids generally showed a higher order parameter when close to a Lipid II molecule, whereas the ADPG molecules generally showed a reduced order parameter close to Lipid II. The ALPG lipid order parameters were unaffected by the distance to Lipid II (data not shown).

Interactions between Plectasin and the *S. aureus* membrane

Given we find that the Lipid II molecule is flexible in terms of its conformation, it seems reasonable to suggest that it interacts with membrane proteins/peptides by either forming rather loose and or non-specific complexes or alternatively more specific, tighter binding

is achieved by reducing the conformational flexibility of Lipid II. The defensin peptide, plectasin is thought to inhibit cell wall biosynthesis by forming stoichiometric complexes with Lipid II. To investigate the nature of the Lipid II-plectasin complex we performed simulations of the complex based on docking studies previously reported by Bonvin and co-workers.[7] Initially, plectasin is complexed to Lipid II and positioned ~5 Å above the plane defined by the phosphate headgroups of the membrane lipids (i.e. AMPG, ALPG and ADPG). Within a few nanoseconds of unrestrained simulation plectasin moves to interact with the membrane surface. Encouragingly we note that plectasin is conformationally stable in this environment. This is exemplified in Figure 9 showing the secondary structure for each residue in plectasin as a function of time from a representative simulation.

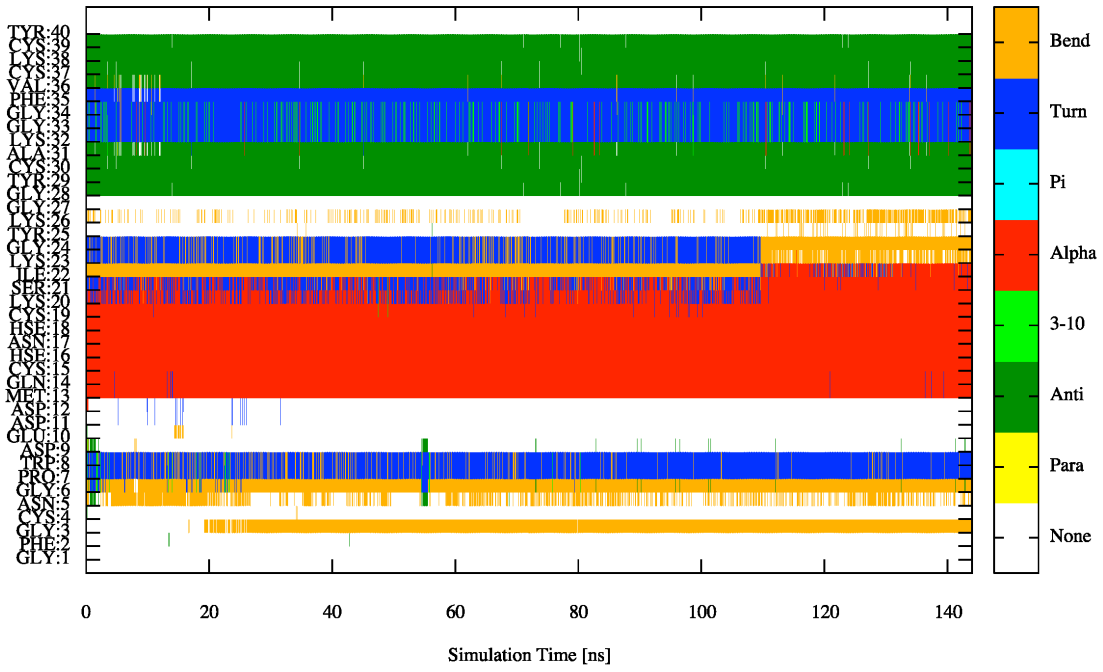

Figure 9 Secondary structure of plectasin-(ε,ε) in a *S. aureus* model membrane. Positional restraints are applied on plectasin and Lipid II for the first 11 ns of the simulations.

The root mean square fluctuation (RMSF) was calculated for each residue of plectasin; representative data are shown in Figure 10. As expected the largest fluctuations are seen for the residues not participating in a defined secondary structure, i.e. the N-terminal

region together with the residues connecting the α-helix and the β-strands. The residues in the α-helix and the β-strands have RMSF values of <1 Å, while the turns between them have RMSF values up to 2 Å. The N-terminal is particularly flexible with RMSF values up to 3.4 Å.

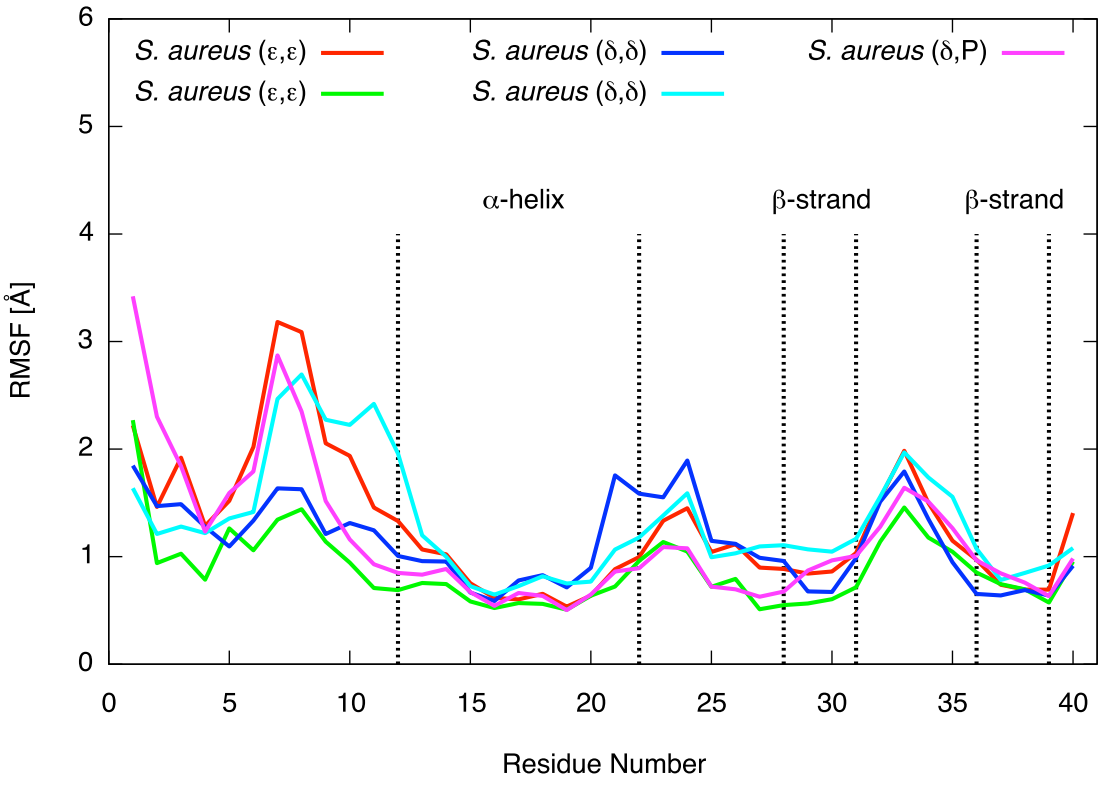

Figure 10 RMSF [Å] values per residue in plectasin calculated for the backbone atoms for selected systems. Indicated in dashed vertical lines are the secondary structure traits found in the original NMR ensemble 1ZFU, which is also seen consistently throughout our simulations, see for instance Figure 9.

During the remainder of the simulation time, plectasin forms a loose aggregate with the membrane and several different binding modes are observed. This is summarised in Figure 11, where it is also seen that the contact mode between plectasin and the membrane depends on the protonation state of the two histidine residues: When the histidines are protonated on the ε-nitrogen (subfigures a) and d)) the contact with the membrane is mainly through the α-helix, whereas in the simulations in which the histidines are protonated on the δ-nitrogen (subfigures b), c) and e)) plectasin interacts with the membrane, predominantly through the residues in the β-sheet. This mode of

contact corresponds approximately to those residues experiencing a change in chemical shift upon titration with DPC micelle in the NMR experiments performed by Schneider *et al.*[7]

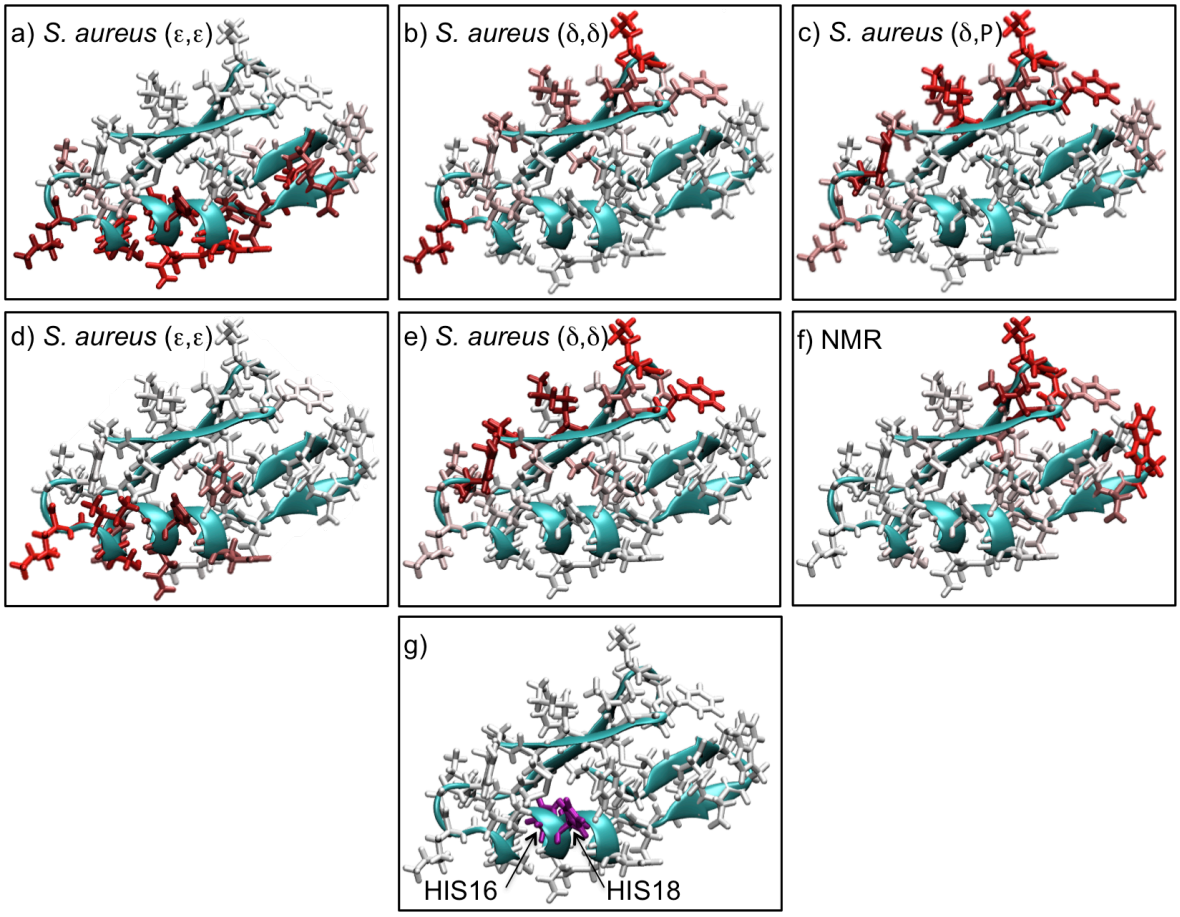

Figure 11 Plectasin. The sidechains are coloured according to the number of contacts (contact is defined as inter-atomic distance ≤ 3.5 Å) made with the membrane; sidechains coloured in red making the most numerous contacts and the sidechains in white making the least: a) *S. aureus* (ε,ε); b) *S. aureus* (δ,δ); c) *S. aureus* (δ,P); d) *S. aureus* (ε,ε); e) *S. aureus* (δ,δ); f) The colour is according to the magnitude in change of chemical shift of the backbone amide protons upon titration with DPC micelles from Schneider *et al.*[7] The residues coloured red are those with the largest change in chemical shift. i) Location of the two histidine residues (coloured purple). The backbone of plectasin is shown in cyan.

Plectasin- Lipid II interactions

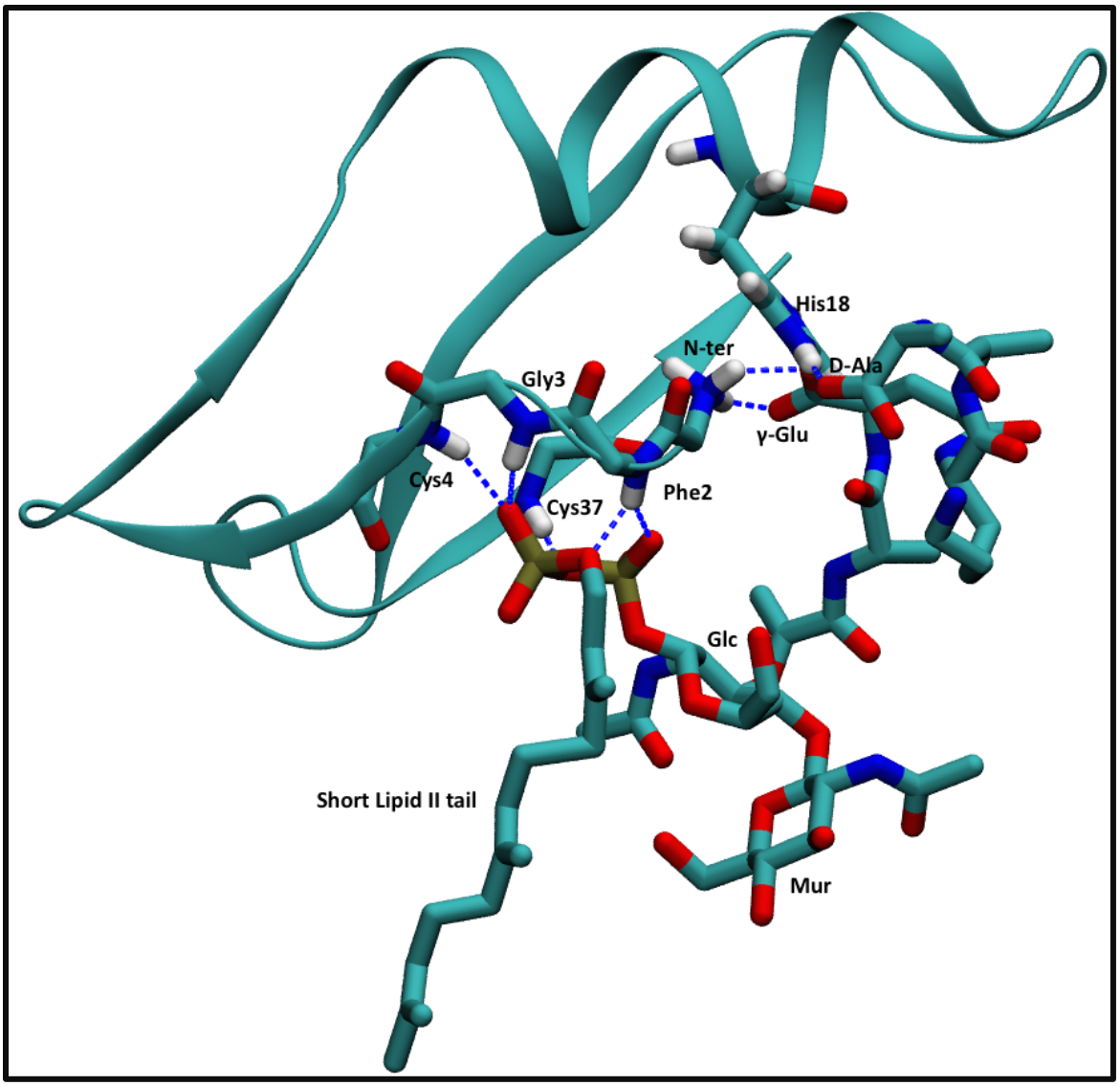

Figure 12 The original plectasin-Lipid II complex[7] with hydrogen bonds and salt-bridges indicated by dashed blue lines. The backbone of plectasin is shown in a cyan cartoon with explicit representation of the backbone atoms of residues Phe2, Gly3, Cys4 and Cys37, the N-terminal amino group and the residue His18 are shown with all atoms as well. The Lipid II molecule is the version with the short tail. All hydrogen atoms are omitted from Lipid II for clarity. The atoms are coloured according to cyan-carbon, white-hydrogen, red-oxygen, tan-phosphorous and blue-nitrogen.

The original plectasin-Lipid II complex[7] was defined by hydrogen bonds between the backbone amide-proton on Phe2, Gly3, Cys4 and Cys37 to several of the monovalent oxygens in the pyrophosphate group in Lipid II. In addition, salt-bridges were found between the carboxylate oxygens of γ-Glu in the penta-peptide chain of Lipid II and to the protonated amino group at the N-terminus and to the protonated His18 of plectasin, see Figure 12.

Our simulations suggest that the protein and Lipid II are only loosely associated in the docked complex. We observed several rather labile hydrogen bonds between the protein and Lipid II, but we only observe the hydrogen bonds between Phe2, Gly4, Cys4 and Cys37 and the pyrophosphate oxygens when either positional restraints are applied to the full plectasin-Lipid II complex or when these hydrogen bonds are reinforced by distance restraints between those atoms involved in the hydrogen bonding. However, in simulations these hydrogen bonds were disrupted within a few nanoseconds after removal of the restraints. The N-terminal hydrogens of plectasin formed a variety of labile hydrogen bond interactions with the oxygens in Lipid II's pyrophosphate group and sugars and the distal Ala in Lipid II's penta-peptide chain during the simulations with the complex in the *S. aureus* model membrane. The oxygen atoms on the γ-Glu in Lipid II, did on the other hand, form changing contacts to both Lys38 and His18 in plectasin. These contacts were of varying lifetime dependent on the system in question, for other systems these interactions were not seen at all. In one of the *S. aureus* (δ,δ) systems Lys38 formed persistent hydrogen bonds to the Lipid II pyrophosphate group and proximate sugar, while in one of the *S. aureus* (ε,ε) systems Lys38 formed stable contact to the distal Ala of the penta-peptide chain.

Discussion

Our simulation study provides the first reported computational study of Lipid II, an important precursor of the bacterial cell wall component, peptidoglycan, in a complex membrane model comprised of multiple lipid types. In this paper we describe an atomistic molecular dynamics study of the conformational dynamics of Lipid II in a model *S. aureus* membrane. In addition, we also investigate how this lipid interacts with the defensin peptide, plectasin. Our simulations reveal that even within the confines of the membrane, Lipid II is a flexible molecule, which is able to adopt a range of different conformations. The terminal methyl group of the Lipid II tail is not located in one region of the hydrophobic core of the membrane, but instead during the course of each simulation it is found in multiple locations that span the hydrophobic width of the membrane (Figure 2) this is in agreement with a similar study reported by Chugunov *et al*.[30] In the process of peptidoglycan synthesis, flip-flop of Lipid II across the bacterial membrane is a critical step. The conformational freedom of the Lipid II tail shows that it is indeed the flipping of the hydrophilic head group that would require active translocation while the tail itself would follow with no energy penalty. In addition, the head group of Lipid II also displays a high degree of conformational freedom with the two sugar rings roaming freely in the bilayer/water interface. As the remainder of Lipid II, the pentapeptide is also flexible adopting a wide range of conformations. The distal residues in this chain are completely exposed in the solvent and thus interactions with glycopeptides such as Vancomycin can supposedly occur without any energy penalty.

On the timescale of our simulations the presence of Lipid II does have some impact upon the disordering of the other lipids in the membrane. The structural properties of the *S. aureus* membrane are largely unaltered both by the incorporation of one or two Lipid II molecules. However, we do observe partitioning of specific lipid types around the Lipid II molecule. The local concentration of ALPG increases during the course of the simulations, and this lipid is most often in contact with Lipid II. This may be due to the increased availability of potential hydrogen-bonding because of the charged lysyl moieties on the ALPG headgroup.

Interestingly, in one simulation we observed a stable dimerization of two Lipid II molecules mediated by a sodium ion coordinating to the pyrophosphate groups on both

Lipid II molecules. We note that Lipid II dimerization may be important for the formation of pores by the lantbiotic nisin as experimental studies have shown that 8 nisin peptides form a pore together with 4 Lipid II molecules.[49]

Lipid II forms loose associations in multiple binding models with the defensin peptide plectasin, and the complex structure proposed by Schneider *et al*.[7] is not stable in our simulations. This could be a consequence of the docked complex being modelled without lipids or detergents present, which would make the pyrophosphate group more accessible for interactions. In our simulations, the pyrophosphate group is buried in the bilayer interface. The use of a truncated Lipid II tail may possibly allow for a more accessible binding region on the Lipid II head group. Our simulations of the full Lipid II tail have shown full extension of the tail into the opposite lipid leaflet, and may result in the Lipid II plectasin-binding region being more 'buried'.

In the systems with the *S. aureus* model membrane plectasin displays a significantly different binding mode depending on the protonation state of the two histidine residues. The altered histidine protonation profile causes a change in the electrostatic interactions with the membrane such that protonation of the ε-nitrogen atoms of His16 and His18, which are located in the α-helix, induces membrane interactions with the helix. In contrast, when the δ-nitrogen atoms are protonated, the membrane interactions are preferentially with the beta strands of plectasin. This may suggest a mechanism for controlling the orientation of the protein with respect to the membrane, although further simulation and experimental studies would be required to explore this in greater depth. A clear strength of our study is the inclusion of lipids that more accurately represent the *S. auerus* cell membrane than just simple phospholipids. However while we include relevant biochemical details of the membrane there are still areas that may be improved. If we reflect upon the limitations of the current study, then it is clear that as with the vast majority of atomistic simulations of biological membranes, it is desirable to access much longer timescales. For example longer simulations would enable us to more fully explore the dimerization of Lipid II, which could potentially lead to more stable complexes with plectasin. Given the limitations inherent to atomistic simulations, this argues for coarse-grain models of Lipid II and the *S. aureus* membrane for multi-scale studies in the future. Nevertheless, here we have been able to show that even on timescales of hundreds of

nanoseconds, Lipid II is a conformationally flexible molecule that interacts with plectasin in a non-specific way, and can alter its local membrane environment.

Acknowledgements

The authors acknowledge helpful discussions with Samuel Genheden and Richard Bradshaw and the use of the Iridis3 and Iridis4 supercomputers at the University of Southampton, and the CAB and SIERRA supercomputers at Lawrence Livermore National Laboratory. We thank the Livermore Computing Grand Challenge for computer time. We acknowledge financial support from DeIC - Danish e-Infrastructure Cooperation and the Lundbeck Foundation. Portions of this work were performed under the auspices of the US Department of Energy by Lawrence Livermore National Laboratory under Contract DE-AC52-07NA27344, Release LLNL-JRNL-xxxxxx.

References

(1) Schneider, T., and Sahl, H.-G. (2010) An oldie but a goodie - cell wall biosynthesis as antibiotic target pathway. *Int. J. Med. Microbiol. 300*, 161–169.
(2) Walsh, C. T., Fisher, S. L., Park, I. S., Prahalad, M., and Wu, Z. (1996) Bacterial resistance to vancomycin: five genes and one missing hydrogen bond tell the story. *Chem. Biol. 3*, 21–28.
(3) Hsu, S.-T. D., Breukink, E., Tischenko, E., Lutters, M. A. G., de Kruijff, B., Kaptein, R., Bonvin, A. M. J. J., and van Nuland, N. A. J. (2004) The nisin-lipid II complex reveals a pyrophosphate cage that provides a blueprint for novel antibiotics. *Nat. Struct. Mol. Biol. 11*, 963–967.
(4) Ling, L. L., Schneider, T., Peoples, A. J., Spoering, A. L., Engels, I., Conlon, B. P., Mueller, A., Schäberle, T. F., Hughes, D. E., Epstein, S., Jones, M., Lazarides, L., Steadman, V. A., Cohen, D. R., Felix, C. R., Fetterman, K. A., Millett, W. P., Nitti, A. G., Zullo, A. M., Chen, C., and Lewis, K. (2015) A new antibiotic kills pathogens without detectable resistance. *Nature 517*, 455–459.
(5) Mygind, P. H., Fischer, R. L., Schnorr, K. M., Hansen, M. T., Sönksen, C. P., Ludvigsen, S., Raventós, D., Buskov, S., Christensen, B., De Maria, L., Taboureau, O., Yaver, D., Elvig-Jørgensen, S. G., Sørensen, M. V., Christensen, B. E., Kjærulff, S., Frimodt-Moller, N., Lehrer, R. I., Zasloff, M., and Kristensen, H.-H. (2005) Plectasin is a peptide antibiotic with therapeutic potential from a saprophytic fungus. *Nature 437*, 975–980.
(6) Brinch, K. S., Sandberg, A., Baudoux, P., Van Bambeke, F., Tulkens, P. M., Frimodt-Moller, N., Høiby, N., and Kristensen, H.-H. (2009) Plectasin shows intracellular activity against Staphylococcus aureus in human THP-1 monocytes and in a mouse peritonitis model. *Antimicrob. Agents Chemother. 53*, 4801–4808.
(7) Schneider, T., Kruse, T., Wimmer, R., Wiedemann, I., Sass, V., Pag, U., Jansen, A., Nielsen, A. K., Mygind, P. H., Raventós, D. S., Neve, S., Ravn, B., Bonvin, A. M. J. J., De Maria, L., Andersen, A. S., Gammelgaard, L. K., Sahl, H.-G., and Kristensen, H.-H. (2010) Plectasin, a fungal defensin, targets the bacterial cell wall precursor Lipid II. *Science 328*, 1168–1172.
(8) Mandal, K., Pentelute, B. L., Tereshko, V., Thammavongsa, V., Schneewind, O., Kossiakoff, A. A., and Kent, S. B. H. (2009) Racemic crystallography of synthetic protein enantiomers used to determine the X-ray structure of plectasin by direct methods. *Protein Sci. 18*, 1146–1154.
(9) Jorgensen, W. L., Chandrasekhar, J., Madura, J. D., Impey, R. W., and Klein, M. L. (1983) Comparison of simple potential functions for simulating liquid water. *J. Chem. Phys. 79*, 926–935.
(10) Wu, E. L., Cheng, X., Jo, S., Rui, H., Song, K. C., Dávila-Contreras, E. M., Qi, Y., Lee, J., Monje-Galvan, V., Venable, R. M., Klauda, J. B., and Im, W. (2014) CHARMM-GUI Membrane Builder toward realistic biological membrane simulations. *J. Comput. Chem. 35*, 1997–2004.
(11) Piggot, T. J., Holdbrook, D. A., and Khalid, S. (2011) Electroporation of the E. coli and S. Aureus membranes: molecular dynamics simulations of complex bacterial membranes. *J. Phys. Chem. B 115*, 13381–13388.
(12) Gould, R. M., and Lennarz, W. J. (1970) Metabolism of Phosphatidylglycerol and

Lysyl Phosphatidylglycerol in Staphylococcus aureus. *J. Bacteriol. 104*, 1135–1144.
(13) Haest, C., De Gier, J., and Op Den Kamp, J. A. F. (1972) Changes in permeability of Staphylococcus aureus and derived liposomes with varying lipid composition. *BBA-Biomembranes 255*, 720–733.
(14) White, D. C., and Frerman, F. E. (1968) Fatty acid composition of the complex lipids of Staphylococcus aureus during the formation of the membrane-bound electron transport system. *J. Bacteriol. 95*, 2198–2209.
(15) Best, R. B., Zhu, X., Shim, J., Lopes, P. E. M., Mittal, J., Feig, M., and Alexander D MacKerell, A., Jr. (2012) Optimization of the Additive CHARMM All-Atom Protein Force Field Targeting Improved Sampling of the Backbone ϕ, ψ and Side-Chain $\chi1$ and $\chi2$ Dihedral Angles. *J. Chem. Theory Comput. 8*, 3257–3273.
(16) Mackerell, A. D., Feig, M., and Brooks, C. L. (2004) Improved treatment of the protein backbone in empirical force fields. *J. Am. Chem. Soc. 126*, 698–699.
(17) MacKerell, A. D., Bashford, D., Bellott, M., Dunbrack, R. L., Evanseck, J. D., Field, M. J., Fischer, S., Gao, J., Guo, H., Ha, S., Joseph-McCarthy, D., Kuchnir, L., Kuczera, K., Lau, F. T., Mattos, C., Michnick, S., Ngo, T., Nguyen, D. T., Prodhom, B., Reiher, W. E., Roux, B., Schlenkrich, M., Smith, J. C., Stote, R., Straub, J., Watanabe, M., Wiórkiewicz-Kuczera, J., Yin, D., and Karplus, M. (1998) All-atom empirical potential for molecular modeling and dynamics studies of proteins. *J. Phys. Chem. B 102*, 3586–3616.
(18) Klauda, J. B., Venable, R. M., Freites, J. A., O'Connor, J. W., Tobias, D. J., Mondragon-Ramirez, C., Vorobyov, I., Mackerell, A. D., and Pastor, R. W. (2010) Update of the CHARMM all-atom additive force field for lipids: validation on six lipid types. *J. Phys. Chem. B 114*, 7830–7843.
(19) Vanommeslaeghe, K., Hatcher, E., Acharya, C., Kundu, S., Zhong, S., Shim, J., Darian, E., Guvench, O., Lopes, P., Vorobyov, I., and MacKerell, A. D. (2010) CHARMM general force field: A force field for drug-like molecules compatible with the CHARMM all-atom additive biological force fields. *J. Comput. Chem. 31*, 671–690.
(20) Beglov, D., and Roux, B. (1994) Finite representation of an infinite bulk system: Solvent boundary potential for computer simulations. *J. Chem. Phys. 100*, 9050–9063.
(21) Guvench, O., Greene, S. N., Kamath, G., Brady, J. W., Venable, R. M., Pastor, R. W., and Mackerell, A. D. (2008) Additive empirical force field for hexopyranose monosaccharides. *J. Comput. Chem. 29*, 2543–2564.
(22) Guvench, O., Hatcher, E. R., Venable, R. M., Pastor, R. W., and Mackerell, A. D. (2009) CHARMM Additive All-Atom Force Field for Glycosidic Linkages between Hexopyranoses. *J. Chem. Theory Comput. 5*, 2353–2370.
(23) Guvench, O., Mallajosyula, S. S., Raman, E. P., Hatcher, E., Vanommeslaeghe, K., Foster, T. J., Jamison, F. W., and Mackerell, A. D. (2011) CHARMM additive all-atom force field for carbohydrate derivatives and its utility in polysaccharide and carbohydrate-protein modeling. *J. Chem. Theory Comput. 7*, 3162–3180.
(24) Mallajosyula, S. S., and Mackerell, A. D. (2011) Influence of solvent and intramolecular hydrogen bonding on the conformational properties of o-linked glycopeptides. *J. Phys. Chem. B 115*, 11215–11229.
(25) Hsu, S. T., Breukink, E., de Kruijff, B., and Kaptein, R. (2002) Mapping the targeted membrane pore formation mechanism by solution NMR: the nisin Z and lipid II interaction in SDS micelles. *Biochemistry 41*, 7670–7676.

(26) Breukink, E., and Ben de Kruijff. (2006) Lipid II as a target for antibiotics. *Nat. Rev. Drug Discov. 5*, 321–323.
(27) van Heijenoort, J. (2007) Lipid intermediates in the biosynthesis of bacterial peptidoglycan. *Microbiol. Mol. Biol. Rev. 71*, 620–635.
(28) de Kruijff, B., van Dam, V., and Breukink, E. (2008) Lipid II: A central component in bacterial cell wall synthesis and a target for antibiotics. *Prostag. Leukotr. Ess. 79*, 117–121.
(29) Jia, Z., O'Mara, M. L., Zuegg, J., Cooper, M., and Mark, A. (2013) Erratum: The effect of environment on the recognition and binding of vancomycin to native and resistant forms of lipid II (Biophysical Journal (2011) 101 (2684-2692)). *Biophys. J. 104*, 516–516.
(30) Chugunov, A. O., Pyrkova, D., Nolde, D., Polyansky, A., Pentkovsky, V., and Efremov, R. (2013) Lipid-II forms potential "landing terrain" for lantibiotics in simulated bacterial membrane. *Sci Rep 3*, 1678.
(31) Huang, C.-Y., Shih, H.-W., Lin, L.-Y., Tien, Y.-W., Cheng, T.-J. R., Cheng, W.-C., Wong, C.-H., and Ma, C. (2012) Crystal structure of Staphylococcus aureus transglycosylase in complex with a lipid II analog and elucidation of peptidoglycan synthesis mechanism. *Proc. Natl. Acad. Sci. U.S.A. 109*, 6496–6501.
(32) Jia, Z., O'Mara, M. L., Zuegg, J., Cooper, M. A., and Mark, A. E. (2011) The effect of environment on the recognition and binding of vancomycin to native and resistant forms of lipid II. *Biophys. J. 101*, 2684–2692.
(33) Schneider, T., Senn, M. M., Berger-Bächi, B., Tossi, A., Sahl, H.-G., and Wiedemann, I. (2004) In vitro assembly of a complete, pentaglycine interpeptide bridge containing cell wall precursor (lipid II-Gly5) of Staphylococcus aureus. *Mol. Microbiol. 53*, 675–685.
(34) Humphrey, W., Dalke, A., and Schulten, K. (1996) VMD: visual molecular dynamics. *J. Mol. Graph. Model. 14*, 33–38.
(35) Schneider, T., Kruse, T., Wimmer, R., Wiedemann, I., Sass, V., Pag, U., Jansen, A., Nielsen, A. K., Mygind, P. H., Raventos, D. S., Neve, S., Ravn, B., Bonvin, A. M. J. J., De Maria, L., Andersen, A. S., Gammelgaard, L. K., Sahl, H. G., and Kristensen, H. H. (2010) Plectasin, a Fungal Defensin, Targets the Bacterial Cell Wall Precursor Lipid II. *Science 328*, 1168–1172.
(36) Søndergaard, C. R., and Olsson, M. (2011) Improved treatment of ligands and coupling effects in empirical calculation and rationalization of pK_a values. *J. Chem. Theory Comput. 7*, 2284–2295.
(37) Olsson, M. H. M., Søndergaard, C. R., Rostkowski, M., and Jensen, J. H. (2011) PROPKA3: Consistent Treatment of Internal and Surface Residues in Empirical pKa Predictions. *J. Chem. Theory Comput. 7*, 525–537.
(38) Case, D. A., Darden, T. A., Cheatham, T. E., III, Simmerling, C., Wang, J., Duke, R. E., Luo, R., Walker, R. C., Zhang, W., Merz, K. M., Roberts, B., Hayik, S., Roitberg, A., Seabra, G., Swails, J., Götz, A. W., Kolossváry, I., Wong, K. F., Paesani, F., Vanicek, J., Wolf, R. M., Liu, J., Wu, X., Brozell, S. R., Steinbrecher, T., Gohlke, H., Cai, Q., Ye, X., Wang, J., Hsieh, M.-J., Cui, G., Roe, D. R., Mathews, D. H., Seetin, M. G., Salomon-Ferrer, R., Sagui, C., Babin, V., Luchko, T., Gusarov, S., Kovalenko, A., and A, K. P. AMBER 12. University of California, San Francisco.
(39) Case, D. A., Babin, V., Berryman, J., Betz, R. M., Cai, Q., Cerutti, D. S., Cheatham,

T. E., III, Darden, T. A., Duke, R. E., Gohlke, H., Goetz, A. W., Gusarov, S., Homeyer, N., Janowski, P., Kaus, J., Kolossváry, I., Kovalenko, A., Lee, T. S., LeGrand, S., Luchko, T., Luo, R., Madej, B., Merz, K. M., Paesani, F., Roe, D. R., Roitberg, A., Sagui, C., Salomon-Ferrer, R., Seabra, G., Simmerling, C., Smith, W., Swails, J., Walker, R. C., Wang, J., Wolf, R. M., Wu, X., and Kollman, P. A. (2014) AMBER 14. University of California, San Francisco.
(40) Phillips, J. C., Braun, R., Wang, W., Gumbart, J., Tajkhorshid, E., Villa, E., Chipot, C., Skeel, R. D., Kalé, L., and Schulten, K. (2005) Scalable molecular dynamics with NAMD. *J. Comput. Chem. 26*, 1781–1802.
(41) Crowley, M. F., and Williamson, M. J. (2009) CHAMBER: Comprehensive support for CHARMM force fields within the AMBER software. *Int. J. Quantum Chem.* (Öhrn, Y., and Sabin, J. R., Eds.) *109*, 3767–3772.
(42) Berendsen, H., and Postma, J. (1984) Molecular dynamics with coupling to an external bath. *J. Chem. Phys. 81*, 3684–3690.
(43) Pastor, R. W., Brooks, B. R., and Szabo, A. (1988) An analysis of the accuracy of Langevin and molecular dynamics algorithms. *Mol. Phys. 65*, 1409–1419.
(44) Ryckaert, J.-P., Ciccotti, G., and Berendsen, H. J. C. (1977) Numerical integration of the cartesian equations of motion of a system with constraints: molecular dynamics of n-alkanes. *J. Comput. Phys. 23*, 327–341.
(45) Darden, T. A., York, D., and Pedersen, L. (1993) Particle mesh Ewald: An N▪ log (N) method for Ewald sums in large systems. *J. Chem. Phys. 98*, 10089–10092.
(46) Martyna, G. J., Tobias, D. J., and Klein, M. L. (1994) Constant pressure molecular dynamics algorithms. *J. Chem. Phys. 101*, 4177–4189.
(47) Feller, S. E., Zhang, Y., and Pastor, R. W. (1995) Constant pressure molecular dynamics simulation: the Langevin piston method. *J. Chem. Phys. 103*, 4613.
(48) Roe, D. R., and Thomas E Cheatham, I. (2013) PTRAJ and CPPTRAJ: Software for Processing and Analysis of Molecular Dynamics Trajectory Data. *J. Chem. Theory Comput. 9*, 3084–3095.
(49) Hasper, H. E., de Kruijff, B., and Breukink, E. (2004) Assembly and stability of nisin-lipid II pores. *Biochemistry 43*, 11567–11575.